Open access • Journal Article • DOI:10.1093/CVR/CVAA088

Sustained subcutaneous delivery of secretome of human cardiac stem cells promotes cardiac repair following myocardial infarction. — Source link

Andrew R Kompa, Andrew R Kompa, David W. Greening, David W. Greening ...+18 more authors

Institutions: University of Melbourne, Monash University, La Trobe University, Baker IDI Heart and Diabetes Institute ...+5 more institutions

Published on: 22 Feb 2021 - Cardiovascular Research (Cardiovasc Res)

Topics: Stem cell

CVR-2019-1027

Sustained subcutaneous delivery of secretome of human cardiac stem cells promotes cardiac repair following myocardial infarction

Andrew R. Kompa[1,2*], David W. Greening[3,4*], Anne M. Kong[5*], Paul J. McMillan[6], Hoayun Fang[3], Ritika Saxena[5,7], Raymond C.B. Wong[1,8,9], Jarmon G. Lees[1,5], Priyadharshini Sivakumaran[5], Andrew E. Newcomb[10], Bakhos A. Tannous[11,12], Cameron Kos[13], Lina Mariana[13], Thomas Loudovaris[13], Derek J. Hausenloy[14,15,16,17,18,19#], Shiang Y. Lim[1,5#]

[1]Departments of Medicine and Surgery, University of Melbourne, Victoria, Australia.

[2]Centre of Cardiovascular Research and Education in Therapeutics, Department of Epidemiology and Preventive Medicine, Monash University, Victoria, Australia.

[3]Baker Heart and Diabetes Institute, Melbourne, Victoria, Australia.

[4]La Trobe Institute for Molecular science, La Trobe University, Melbourne, Victoria, Australia.

[5]O'Brien Institute Department, St Vincent's Institute of Medical Research, Victoria, Australia.

[6]Department of Biochemistry and Molecular Biology, Biological Optical Microscopy Platform, University of Melbourne, Victoria, Australia.

[7]Deakin University, Victoria, Australia.

[8]Centre for Eye Research Australia, Royal Victorian Eye and Ear Hospital, East Melbourne, Victoria, Australia.

[9]Shenzhen Eye Hospital, Shenzhen University School of Medicine, Shenzhen, China.

[10]Department of Cardiothoracic Surgery, St Vincent's Hospital Melbourne, Victoria, Australia.

[11]Department of Neurology and Pathology, Massachusetts General Hospital, Charlestown, Massachusetts, USA.

[12]Program in Neuroscience, Harvard Medical School, Boston, Massachusetts, USA.

[13]St Vincent's Institute of Medical Research, Victoria, Australia.

[14]Cardiovascular and Metabolic Disorders Program, Duke-National University of Singapore Medical School, Singapore.

[15]National Heart Research Institute Singapore, National Heart Centre, Singapore.

[16]Technologico de Monterrey, Centro de Biotecnologica-FEMSA, Nuevo Leon, Mexico.

[17]Hatter Cardiovascular Institute, University College London, London, UK.

[18]The National Institute of Health Research University College London Hospitals Biomedical Research Centre, UK

[19]Yong Loo Lin School of Medicine, National University Singapore, Singapore.

[*]Equally contributing authors

[#]Joint senior authors, both contributed equally to this work.

Running Title:

Cardiac repair with cardiac stem cell secretome

Word count:

4757

Corresponding author:

Shiang Y. Lim, Ph.D.

O'Brien Institute Department, St Vincent's Institute of Medical Research,

9 Princes Street, Fitzroy, Victoria 3065, Australia.

Tel : +613 9231 4020

Fax : +613 9416 2676

Email : maxlim@unimelb.edu.au; mlim@svi.edu.au

ABSTRACT

Aims: To establish pre-clinical proof of concept that sustained subcutaneous delivery of the secretome of human cardiac stem cells (CSCs) can be achieved *in vivo* to produce significant cardioreparative outcomes in the setting of myocardial infarction.

Methods and Results: Rats were subjected to permanent ligation of left anterior descending coronary artery and randomized to receive subcutaneous implantation of TheraCyte devices containing either culture media as control or $1x10^6$ human $W8B2^+$ CSCs, immediately following myocardial ischaemia. At 4 weeks following myocardial infarction, rats treated with $W8B2^+$ CSCs encapsulated within the TheraCyte device showed preserved left ventricular ejection fraction. The preservation of cardiac function was accompanied by reduced fibrotic scar tissue, interstitial fibrosis, cardiomyocyte hypertrophy, as well as increased myocardial vascular density. Histological analysis of the TheraCyte devices harvested at 4 weeks post-implantation demonstrated survival of human $W8B2^+$ CSCs within the devices, and the outer membrane was highly vascularized by host blood vessels. Using CSCs expressing plasma membrane reporters, extracellular vesicles of $W8B2^+$ CSCs were found to be transferred to the heart and other organs at 4 weeks post-implantation. Furthermore, mass spectrometry-based proteomic profiling of extracellular vesicles of $W8B2^+$ CSCs identified proteins implicated in inflammation, immunoregulation, cell survival, angiogenesis, as well as tissue remodelling and fibrosis that could mediate the cardioreparative effects of secretome of human $W8B2^+$ CSCs.

Conclusions: Subcutaneous implantation of TheraCyte devices encapsulating human $W8B2^+$ CSCs attenuated adverse cardiac remodelling and preserved cardiac function following myocardial infarction. The TheraCyte device can be employed to deliver stem cells in a minimally invasive manner for effective secretome-based cardiac therapy.

Keywords: Myocardial infarction; Cardiac stem cells; TheraCyte; Secretome; Heart Failure; Cardiac remodelling

TRANSLATIONAL PERSEPCTIVE (100 words)

The recognition that cardioreparative effects of adult stem cells are attributed to their salutary paracrine activity is driving the recent paradigm shift to harness stem cell paracrine effects for effective cardiac repair. However, poor cell engraftment post-transplantation limits the release of paracrine factors over time and thus their therapeutic efficacy. This study demonstrates sustained delivery of the secretome from cardiac stem cells using an immune-isolation device, implanted subcutaneously, to produce cardioreparative effects following myocardial infarction. This innovative delivery method is minimally invasive and clinically adaptable for other stem cell types with a high secretory profile and for other cardiovascular diseases.

INTRODUCTION

Heart failure following myocardial infarction (MI) is one of the leading causes of death and disability worldwide.[1] Therapeutic strategies for repairing the heart to prevent adverse left ventricular remodelling and reduce the risk of heart failure following MI are an important unmet clinical need. Stem cell-based therapy has great potential for the repair of ischaemic hearts, and the beneficial effects on cardiac function and structure have been mainly attributed to the secretome of the transplanted stem cells, rather than the ability of adult stem cells to form functional cardiomyocytes in the infarcted myocardium.[2] However, current clinically relevant cell delivery routes such as intramyocardial injection, are invasiveness and suffer from poor cell retention. Direct delivery of cells into heart tissue is associated with significant cell loss through the needle track and a high degree of cell death in the harsh ischaemic cardiac milieu.[3] However, it may not be necessary for the cells to be injected into the infarcted myocardium to harness their beneficial effects of their secretomes, given that stem cells can exert their cardioreparative effects distally by secreting paracrine factors (especially via extracellular vesicles [EVs] which protect these factors from degradation) into the circulation.[4, 5] While this can be achieved by the minimally invasive intravascular route, cells delivered via this method become trapped in the lung and are eventually cleared from the body by the immune system over several days.[5] This means that the beneficial paracrine effects of transplanted cells, delivered using these conventional methods, are short-lived and this has been the 'bottleneck' to realisation of the full potential of stem cell-based therapy. Therefore, a major challenge in leveraging the paracrine signalling mechanisms of stem cells to stimulate endogenous cardiac repair is the efficient, sustainable, and minimally invasive delivery of their secretome to the myocardium.

Here, we present an innovative methodology to deliver subcutaneously the secretome of cardiac stem cells (CSCs) in a sustained and minimally invasive manner using an immune-isolation device, TheraCyte, for cardioreparative therapy post-MI. The TheraCyte device has a bilaminar membrane

system: an inner membrane to protect encapsulated cells from the host's immune system while allowing nutritional inputs and therapeutic outputs, and an outer membrane that promotes blood vessel formation to facilitate the exchange of oxygen, nutrients and secretome (*Figure 1A*). Our previous studies have demonstrated that human W8B2$^+$ CSCs secrete a myriad of bioactive paracrine factors that can be harnessed for therapeutic use in cardiac repair.[6, 7] In this proof-of-concept study, we have shown that subcutaneous implantation of TheraCyte device encapsulating the human W8B2$^+$ CSCs prevented adverse cardiac remodelling and preserved cardiac function at 4 weeks post-MI in rats. This clinically adaptable cell delivery approach offers the opportunity to harness the paracrine-mediated benefits of transplanted cells in a sustained, controllable, reversible and safe manner.

METHODS

A detailed description of the methods used in this study is provided in Supplementary material online.

Human W8B2$^+$ cardiac stem cells

Human tissue sample collection was approved by the Human Research Ethics Committee-A of St. Vincent's Hospital (HREC-A07/08) and the present study complies with the Declaration of Helsinki. Informed written consent was given prior to the inclusion of subjects in the study. Freshly excised specimens of atrial appendages were collected from consented adult patients who underwent coronary artery bypass grafting surgery, and W8B2$^+$ CSCs were isolated as previously described.[6]

Extracellular vesicle reporter cells

Human W8B2$^+$ CSCs were transduced with lentiviruses expressing GlucB and GFP separated by an internal ribosomal entry site (CSCW-GlucB-IRES-GFP) and a similar vector expressing sshBirA

and mCherry (CSCW-sshBirA-IRES-mCherry).[8] Cells expressing both GFP and mCherry fluorescence were sorted using flow cytometry (FACSAria, BD Biosciences, USA).

Cell encapsulation

TheraCyte devices (TheraCyte, CA, USA) with 20 µL loading volume were conditioned in 95% v/v ethanol for 10 min, 20% v/v ethanol for 10 min and rinsed in sterile phosphate buffered saline in sequential order. The conditioned TheraCyte devices were loaded with either $1x10^6$ human $W8B2^+$ CSCs (passage 2-3) suspended in 20 µL of growth media or 20 µL of growth media alone (as control) using a Hamilton syringe. The cell loading port was then sealed with medical grade adhesive silicone, type A (Nusil, CA, USA) and the excess port was trimmed off. The device was then placed in growth media at 37°C in a humidified 5% carbon dioxide incubator for 2-3 days before implantation.

Myocardial infarction

Experimental procedures were approved by the Animal Ethics Committee of St Vincent's Hospital and were conducted in accordance with the Australian National Health and Medical Research Council guidelines for the care and use of laboratory animals (AEC No. 001/17). All animal procedures conformed to the guidelines from Directive 2010/63/EU of the European Parliament on the protection of animals used for scientific purposes or the NIH guidelines. Adult male nude rats aged 13-16 weeks (Animal Resources Centre, WA, Australia), weighing between 200-307 g were anaesthetized with a single bolus dose of alfaxalone (15 mg/kg, intravenously), intubated and maintenance anaesthesia was provided with 2% isoflurane in oxygen at 70-75 breaths per minute. Through a left anterior thoracotomy, the left anterior descending coronary artery was identified and permanently ligated 2 mm below the left atrium using a 6/0 prolene monofilament polypropylene suture. Successful coronary artery occlusion was confirmed by visible blanching of the myocardium distal to the coronary ligation. The thorax and muscle layers were closed and the animals turned

over for subcutaneous placement of a TheraCyte device containing either human W8B2+ CSCs or media (control) at the dorsal side of the animals. An incision was made at the level of the shoulder blades and a pocket was created by blunt dissection under the skin where the TheraCyte was inserted. The skin wound was closed and a single dose of carprofen (5 mg/kg, subcutaneously) was administered as an analgesic. Transthoracic echocardiography was performed prior to MI under light anaesthesia with spontaneous respiration using isoflurane to evaluate changes in cardiac function using a Vivid 7 Dimension ultrasound imaging machine (GE Vingmed, Horten, Norway) with a 10 MHz phased array probe. At 28 days post-MI and following echocardiographic assessment, the hearts of anaesthetised animals (2% isoflurane in oxygen) were excised and fixed in 4% paraformaldehyde for histological analysis. MI and transthoracic echocardiography were performed and analysed by A.R.K., who was blinded to the treatment allocation.

Statistics

Data are expressed as mean ± SEM. Statistical analysis was performed using GraphPad Prism software with student's t-test where values of $P < 0.05$ were considered statistically significant.

RESULTS

Subcutaneously implanted W8B2$^+$ CSCs encapsulated in a TheraCyte device are cardioprotective

To demonstrate the feasibility and efficacy of using the TheraCyte device to provide sustained subcutaneous delivery of secretome from encapsulated human stem cells as a cardioreparative strategy for MI, a TheraCyte device encapsulating $1x10^6$ human W8B2$^+$ CSCs was subcutaneously implanted into a rat immediately after coronary artery ligation to induce MI. Left ventricular ejection fraction (LVEF) was similar between W8B2$^+$ CSC group and control group before MI and at 1 week post-MI. At 4 weeks post-treatment, implantation of W8B2$^+$ CSCs significantly preserved LVEF while the LVEF in the control group continued to deteriorate ($P < 0.05$, *Figure 1B*). Other

LV function parameters were not significantly different between groups except for a reduced left ventricular internal end-systolic dimension at 4 weeks post-MI, though a trend toward better LV function in W8B2$^+$ CSC group was evident (*Supplementary material online, Table S1*).

The preservation in LV function in the W8B2$^+$ CSC group was accompanied by less cardiac hypertrophy as measured by heart weight over body weight (3.13 ± 0.05 versus 4.07 ± 0.14 in control, $P < 0.05$), smaller infarct scar size (*Figure 1C*), less interstitial fibrosis (*Figure 1D*) and a smaller degree of cardiomyocyte hypertrophy (*Figure 1E*). Moreover, myocardial vascular density, determined by lectin staining for all vessel types and smooth muscle actin staining for arterioles, were significantly increased in rats treated with W8B2$^+$ CSCs (*Figure 1F-G*). Taken together, these data indicate that subcutaneous implantation of W8B2$^+$ CSCs encapsulated in the TheraCyte devices can deliver sustained doses of paracrine factors systemically to improve cardiac function and attenuate adverse cardiac remodelling post-MI.

Encapsulated W8B2$^+$ CSCs survive and proliferate over 4 weeks *in vivo*

To assess influence of encapsulation and *in vivo* implantation on W8B2$^+$ CSCs, histological analysis was performed on TheraCytes harvested at 4 weeks post-implantation. Encapsulated W8B2$^+$ CSCs expanded in number and organized into tissue-like structures within the self-secreted extracellular matrices inside the TheraCyte devices over the 4 weeks duration (*Figure 2A-B*, *Supplementary material online, Figure S1).* The implanted human CSCs remained fully contained within the inner membranes of the TheraCyte devices as demonstrated by the human specific KU80 staining (*Figure 2C*). Immunostaining with the apoptotic cell death marker cleaved caspase-3 (*Figure 2E)* and pan-cell cycle marker Ki67 (*Figure 2E*) showed survival of encapsulated human cells and a small proportion of encapsulated cells remained proliferative (4.07±1.72% Ki67 positive cells) after 4 weeks of implantation, respectively. Although the encapsulation and *in vivo* implantation did not affect the expression of vimentin, a mesenchymal marker strongly expressed

by the W8B2$^+$ CSCs, nor induce CSC differentiation into endothelial lineage as indicated by the negative expression of endothelial cell marker CD31, some of the encapsulated cells did express smooth muscle actin after 4 weeks of implantation (*Supplementary material online, Figure S2A-C*). At 4 weeks post-implantation, the outer membranes of the devices were highly vascularized by the host vasculature as evident by the rodent-specific lectin staining with erythrocytes present within the lumen of the vasculature (*Figure 2D*) and a layer of fibrous capsule can be detected around the outer membranes of the devices (*Supplementary material online, Figure S1*).

Characterisation of extracellular vesicles secreted by human W8B2$^+$ CSCs

Understanding the spatiotemporal distribution of the secretome *in vivo* is important for clinical translation of secretome-based therapeutic intervention. In order to track the secreted EVs, W8B2$^+$ CSCs were co-transduced with two lentiviruses expressing GlucB-IRES-GFP and sshBirA-IRES-mCherry to establish a stable membrane reporter (W8B2$^+$ CSC$^{GlucB+sshBirA}$) which displayed *Gaussia* luciferase (Gluc) and biotin on the surface of cells and EVs (*Figure 3A-3C, Supplementary material online, Figure S3*).[8] The number of EVs secreted from W8B2$^+$ CSC$^{GlucB+sshBirA}$ were significantly increased (n=3, $P < 0.0001$) over 3 days when cultured in 3D format within the TheraCyte device but not when cultured as a 2D monolayer (*Figure 3C-D, Supplementary material online, Figure S4, S6*). EVs secreted by the encapsulated W8B2$^+$ CSC$^{GlucB+sshBirA}$ had a smaller diameter and more homogeneous size range distribution compared to EVs secreted by cells cultured as a 2D monolayer (*Figure 3E-F*). Interestingly, W8B2$^+$ CSC$^{GlucB+sshBirA}$ released a higher amount of EVs ($2.25x10^9 \pm 2.43x10^8$ particle count/mL) than untransduced W8B2$^+$ CSCs ($4.79x10^8 \pm 4.26x10^7$ particle count/mL) (*Figure 3G, Supplementary material online, Figure S4*).

Mass spectrometry-based proteomic analysis was then performed simultaneously on EVs of transduced cells (W8B2$^+$ CSC$^{GlucB+sshBirA}$) (transduced EVs, T EV), EVs of untransduced cells (UnT EV) and matched untransduced cell lysates (UnT Cell) from three independent experiments, and the

respective amount of identified proteins in these different samples was quantified by a label-free (precursor ion density) approach (*Figure 4, Supplementary material online, Table S3*). We asked whether our comparative proteomic analysis (identified in at least two out of three independent experiments) could enable identification of specific markers of EVs. EV-specific markers including tumor susceptibility 101 (*TSG101*), CD63 antigen (*CD63*), tetraspanin CD81 (*CD81*), and programmed cell death 6-interacting protein (*Alix/PDCD6IP*) were among the proteins highly or significantly enriched in EVs in comparison to cells (*Figure 4B-C, Supplementary material online, Table S4-5*).

In addition, we performed comparative analysis of transduced EVs to ensure our reporter (i.e. lentiviral transduction) did not influence EV composition. Comparison between transduced EVs and untransduced EVs showed that the majority of proteins (93%; 3367 proteins; *Figure 4D*) were common to each group, highly similar in expression of specific markers of EVs (*Figure 4C*), and variance (0.96) between both EV groups based on multi-scatter analysis (*Figure 4E*). Further, this also supports the high level of biological similarity and technical reproducibility within untransduced EVs (0.94-0.97; *Figure 4E*). Of note, in proteins identified enriched (FC >0.5, log2) in transduced EVs in comparison to untransduced EVs, several are known to be associated with endocytic membrane fusion (*RABGEF1, RAB8B, SAMD9L*), ubiquitination (*COMMD1*), endosomal trafficking and sorting (*VPS52,,VPS53, CHMP1A, DENND10*) and membrane trafficking (*RAB11FIP5, MOB4, RAB22A, APPL2, BRK1*) based on Gene Ontology functional annotation (*Supplementary material online, Table S6*).

Biodistribution of extracellular vesicles

In culture, when treated with conditioned media collected from 2D cultured W8B2^{+} CSC$^{GlucB+sshBirA}$ for 48 hours, EVs in the conditioned media were taken up by various human cell types found in the heart including cardiomyocytes derived from induced pluripotent stem cells, untransduced W8B2^{+}

CSCs, fibroblasts, primary cardiac microvascular endothelial cells and primary coronary smooth muscle cells (*Supplementary material online, Figure S6*).

To assess the *in vivo* biodistribution of EVs secreted by the encapsulated W8B2$^+$ CSCs, W8B2$^+$ CSC$^{GlucB+sshBirA}$ were encapsulated in the TheraCyte devices and implanted subcutaneously in rats immediately after myocardial infarction. Minimal Gluc signal can be detected in regions corresponding to the heart and lung regions at 1 week post-implantation, and the intestine region at 4 weeks post-implantation. *Ex vivo* imaging of excised organs and tissues confirmed the lack of detectable Gluc signal in the heart, liver, lung, skeletal muscle, kidney and spleen at 4 weeks post-implantation, but the Gluc signal as well as mCherry fluorescence could be detected in the TheraCyte devices encapsulating the W8B2$^+$ CSC$^{GlucB+sshBirA}$ (*Supplementary material online, Figure S7*). Probing with streptavidin-horseradish peroxidase for biotin and GFP showed localization of EVs across the inner membranes of the TheraCyte device and accumulation in extracellular matrices outside the inner membrane (*Figure 5A-B*). Intense biotin staining can also be detected in some of the host cells in close proximity to the TheraCyte device and in the fibrous scar area of the infarcted myocardium (*Figure 5A*, *Supplementary material online, Figure S8A*). Tracking the GFP proteins, which were packaged into secretory vesicles of W8B2$^+$ CSC$^{GlucB+sshBirA}$ (*Supplementary material online, Figure S3*), showed scattered localization of EVs in the scar, infarct border and remote regions of the myocardium (*Supplementary material online, Figure S8B*). Immunostaining with streptavidin and CD63 antibody for biotin and exosomes, respectively, showed localization of EVs in the interstitial space of myocardium and the perivascular region (*Figure 5C-D*, *Supplementary material online, Figure S9*) while some were taken up by cardiomyocytes (*Figure 5C)*. In addition to the heart, EVs of W8B2$^+$ CSC$^{GlucB+sshBirA}$ can also be found in other organs and tissues, including skeletal muscle, lung, liver, spleen and kidney (*Supplementary material online, Figure S10-11*).

Identification of factors associated with cardiac biology and tissue remodelling in EVs.

We next asked whether our comparative proteomic analysis could allow the identification of known components associated with cardiac biology and function in the EVs secreted from untransduced W8B2^{+} CSCs. We performed functional annotation (UniProt, Reactome and KEGG) to reveal specific components associated with inflammation, immunoregulation (e.g., *CEBPB, CEBPD, SERPINB1, RTN4*), cell survival (*FOXK1, ANP32B, PPP5C, SMARCB1, RIPK1*), angiogenesis (*EMC10, ADAM9, SH3BP1*), as well as tissue remodelling and fibrosis (*RCN3, FAP, SMAD3, EPS8L2*) (*Supplementary material online, Table S7*). Of note, angiotensinogen (*AGT*, Serpin A8) and ryanodine receptor 2 (*RYR2*) which are important in vasoconstriction, embryonic heart development and cardiac muscle contraction, were identified. Further, whole genome enrichment analysis (STRING; functional enrichment analysis) revealed specific pathways associated with ROBO receptor signalling (HSA-376176) and NOTCH signalling (HSA-157118) (*Figure 4F-G*).

Cell surface markers – insights into potential mechanisms that drive localisation of EVs to heart

To determine potential mechanisms that drive localisation of EVs in the myocardium, we analysed our EV proteome for marker expression of membrane (plasma) cell surface (UniProt), human cell atlas (plasma membrane expression distribution),[9] and cardiac fibroblast cell surface markers[10] and their association with cardiac function. Based on these stringent expression and annotation, we reported 116 proteins associated with the plasma membrane, cell surface, and cell surface receptor signalling pathways (*Supplementary material online, Table S8*). We also found 11 proteins annotated with the cell surface and having function associated with cardiac biology (e.g., *PDGFRB, NOTCH2*), 87 proteins associated with the plasma membrane and cell surface (subcellular annotation), and 18 proteins associated with the cell surface receptor signalling pathways (e.g., *FADD, IFITM1, PRMT1, DOK1*). A salient finding of EV cargo proteins included 9 proteins co-identified in human cell atlas with known expression of plasma membrane (*ANK3, ITGA3, TRPV2, STX4, CD109, THBS1, MSN, ABCC1, SLC2A1*) and two proteins identified enriched in cardiac

fibroblasts (*SLTM/MET, CDH2*). Thus, several markers of cell surface and specifically associated with cardiac function and cardiac fibroblast cell surface expression were identified in EVs secreted from untransduced W8B2$^+$ CSCs, providing key insights into molecular bias that potentially are involved in EV tropism to the heart.

DISCUSSION

The present study has demonstrated for the first time that subcutaneous implantation of TheraCyte devices encapsulating human W8B2$^+$ CSCs remote from the heart can effectively preserve cardiac function and attenuate adverse cardiac remodelling in a rat model of myocardial infarction, implying secretory paracrine mechanisms of CSCs in driving cardioreparative outcomes. Importantly, this minimally-invasive method of delivery produced an equivalent cardioreparative effect as intramyocardial injection of W8B2$^+$ CSCs.[6] This cell secretome delivery method is highly attractive as it is non-invasive and allows cells to be transplanted in healthy vascularized tissue sites instead of the hostile environment associated with the infarcted myocardium, which can compromise the survival and function of transplanted cells. Moreover, the devices can be used to deliver allogeneic cells without the concern of immune rejection, and is safe as the encapsulated cells can simply be removed using a simple local procedure anytime following a desirable therapeutic duration. In fact, a previous study has reported the feasibility and safety of allogeneic parathyroid tissue implantation in non-immunosuppressed humans with chronic hypoparathyroidism using the TheraCyte device.[11] In that clinical study, encapsulated allogeneic cells survived up to 1 year after implantation of the devices with no sign of infection or inflammation.[11] Similar outcomes were observed in non-immunosuppressed non-human primates implanted with TheraCyte device containing allogeneic fibroblasts.[12] The TheraCyte devices have also been successfully used in rodents to encapsulate other cell types to deliver insulin,[13, 14] parathyroid hormone[15] and erythropoietin[16] in a sustained manner.

The idea of harnessing the stem cell secretome in a sustained manner for cardiac repair has also recently been explored by other groups using different innovative devices. These include the epicardial devices[17, 18] and catheter-based intravascular bioreactors[19] that are capable of protecting the encapsulated cells from host immune attack while allowing sustained released of paracrine factors. However, these devices entailed invasive implantation methods that will limit their clinical applicability. The epicardial devices required open chest surgery to access the implantation site and the foreign body responses toward these devices on the epicardial surface could aggravate adverse remodelling of the infarcted myocardium post-MI.[17, 18] Although delivery of the intravascular bioreactors to the vasculature[19] can be achieved using the minimally invasive percutaneous surgical technique, the high risk of thrombosis as a result of direct contact between the device and blood flow will limit the translatability of this approach in patients.

Vascularisation of the implanted device is a key determinant of the survival of the encapsulated cells as it facilitates the diffusion of oxygen and nutrients from the surrounding host microcirculation as well as allowing the secretome to be delivered into the systemic circulation. In the present study, all implanted devices were fully vascularised at 4 weeks, including the fibrous capsule surrounding the outer membrane of the devices. The biotinylated EV-GlucB system (GlucB+sshBirA) has been shown to be a non-toxic reporter system to accurately monitor EV levels in different organs.[8] Surprisingly, *in vitro*, we demonstrated for the first time that GlucB+sshBirA transduction significantly induced the release of W8B2$^+$ CSC EVs compared to untransduced W8B2$^+$ CSCs. Likewise, W8B2$^+$ CSC$^{GlucB+sshBirA}$ proteomic analyses revealed enrichment of proteins associated with endocytic membrane fusion, ubiquitination, endosomal trafficking and sorting as well as membrane trafficking, suggesting the increase in EVs generation and released from W8B2$^+$ CSC$^{GlucB+sshBirA}$ was a result of an alteration of the exosome biogenesis pathway. We are aware that several different endosomal pathways are responsible for the sorting, trafficking and release of EVs, however the fact we have identified several key elements enriched in the EVVs of

W8B2$^+$ CSC$^{GlucB+sshBirA}$ highlights the diversity of these key pathways and components in this process.

Nevertheless, the identification of similar contents in EVs from untransduced W8B2$^+$ CSCs and W8B2$^+$ CSC$^{GlucB+sshBirA}$ including proteins mediators of inflammation, immunoregulation, cell survival, angiogenesis, as well as tissue remodelling and fibrosis (*Supplementary material online, Table S7*), indicate that EV-mediated cardiac repair function of W8B2$^+$ CSC EVs is not affected by the GlucB+sshBirA transduction on the exosome biogenesis pathway. *In vivo* bioluminescence imaging showing localization of secreted EVs distal from the implanted site might suggest that vascularisation of the grafted TheraCyte device could have occurred as early as 1 week after implantation and contributed to the robust survival of encapsulated W8B2$^+$ CSCs as determined by the absence of cleaved caspase-3 staining. Note that the weak bioluminescence signal detected in the region of the bladder at 4 weeks was likely to be a 'background' signal from the excreted luciferin following intravenous injection. The degree of vascularisation of the grafted TheraCyte device was similar in both control and W8B2$^+$ CSC groups suggesting that the extent of cardioreparative effects are independent of the degree of device vascularisation. Nevertheless, the human W8B2$^+$ CSCs exhibited good growth in the encapsulated device with some of the surviving encapsulated cells remaining proliferative at 4 weeks after implantation. Staining with various mesodermal lineage markers suggest that the subcutaneous environment preserved the mesenchymal phenotype of the encapsulated human W8B2$^+$ CSCs and promoted their differentiation toward the smooth muscle cell lineage. These data demonstrate that human W8B2$^+$ CSCs survived, proliferated and differentiated within the immune-isolated TheraCyte device to protect the infarcted myocardium via a paracrine mechanism.

The secretome of W8B2$^+$ CSCs is complex[7] and the factors responsible for the cardioreparative outcomes remain to be identified. Our previous study has indicated the likelihood that secreted

factors, both soluble proteins and EVs, act in concert to drive the observed cardioreparative outcomes.[7] Moreover, we have shown that the beneficial effects of the W8B2$^+$ CSC secretome were retained in the EV fraction.[7] These EVs contain a cargo of proteins, mRNA and microRNA precursors that are enriched in exosomes and are capable of modulating many of the cellular pathways involved in protein metabolism and cell growth, as well as cellular responses to stress and organisation of the extracellular matrix.[7] In this study, we confirmed the presence of EV-associated bioactive molecules produced by W8B2$^+$ CSCs shown to contain known regulators of inflammation, immunoregulation, cell survival, angiogenesis, as well as tissue remodelling and fibrosis that are required for successful cardiac repair. To determine their specific functional contribution, further studies are needed to selectively delineate the effects of bioactive factors transferred by EVs. Nevertheless, a recent study by Vagnozzi and colleagues have reported that the functional benefit of CSCs is attributed to an acute inflammatory-based intrinsic wound healing response of the infarcted myocardium post-MI.[20] In the *in vivo* setting, we envisage that the EV component is most likely to be important given that the EVs are likely to offer protection of cardioreparative factors in the systemic circulation. EVs isolated from human stem cells have been shown to protect the infarcted myocardium, retaining therapeutic potency equivalent to that of stem cells.[21-24] Moreover, studies have shown that EVs of human induced pluripotent stem cell-derived cardiovascular progenitor cells[25] and cardiosphere-derived cells[26] are endowed with anti-inflammatory properties that modulate the response of monocyte and macrophage in the myocardium to resolve inflammation. Although inhibitors of EV biogenesis and secretion such as GW4869 and spiroepoxide[27, 28] can be used to further validate that EVs secreted from the encapsulated W8B2$^+$ CSCs are responsible for the cardioreparative effect, administration of these inhibitors *in vivo* can systemically affect EV biogenesis and secretion from other tissues and organs that can confound the data interpretation. To overcome this challenge, we used the EV reporter in W8B2$^+$ CSCs to successfully track the secreted EVs in various organs including the infarcted myocardium, and immunostaining with GFP suggested transfer and cellular integration of the EV

cargo into cardiomyocytes. These findings further support the secretory mechanisms of action of W8B2$^+$ CSCs in mediating cardiac repair post-MI.

There are different mechanisms by which EVs may direct tropism and interact with target cells.[29] EVs may act as signaling complexes by direct stimulation of target cells, by transferring surface receptors between cells, and by delivering proteins, mRNA and bioactive lipids into the target cells. Recently, the surfaceome of EVs has been characterized, which has provided insights into the tropism capacity of EVs,[30] such as through various exosomal integrins to mediate organ-specific delivery.[31] We have utilised global cell surface expression and cardiac subcellular membrane studies to correlate key proteins associated within EVs as potential molecular bias for cardiac tropism and cell surface interaction. Such unique approach has provided potential mechanistic insights underlying the cardiac tropism and cardioreparative effects of EVs of W8B2$^+$ CSCs. In our study, the beneficial effect of W8B2$^+$ CSC EVs could be associated with improving angiogenesis via ROBO receptor signaling (HSA-376176)[27] and promoting cell proliferation and angiogenesis by NOTCH signalling (HSA-157118),[28, 32, 33] among others. Thus, highlighting the potentially broad role of the secretory mechanisms of action of W8B2$^+$ CSCs in mediating cardiac repair and angiogenesis post-MI. However, the exact mechanisms underlying the cardiac repair effects W8B2$^+$ CSC EVs warrant further investigation.

In summary, the TheraCyte devices can provide sustained subcutaneous delivery of secretome of stem cells in a non-invasive fashion for cardiac repair in patients with MI, a global unmet medical need. The encapsulation devices can protect the implanted cells from the host immune system and prevent cell escape into the host, thereby offering the opportunity to achieve the cardioreparative effects of stem cell secretome in a controllable, reversible and safe manner. The subcutaneous devices can be simply and minimally-invasively implanted in an outpatient setting under local anaesthesia, and can be removed as required (e.g. after 3 to 6 months when most post-MI cardiac

remodelling has taken place) in a similar manner. Future studies to extend the current findings are warranted in order to progress this promising cell delivery approach toward clinical applications. These include demonstrating efficacy in a large animal MI model and longer-term cardioreparative effects to demonstrate the clinical applicability to acute MI patients, in whom most left ventricular remodelling occurs over the first 12 weeks post-MI. Building on this proof-of-principle study using the human W8B2^{+} CSCs, the quest to identify other sources of stem cells with a high secretory profile and the ability to stimulate endogenous cardiac repair will improve the versatility of this application in a clinical setting.

ACKNOWLEDGEMENTS

This work was performed with support from the St Vincent's Hospital (Melbourne) Research Endowment Fund and Stafford Fox Medical Research Foundation. Derek Hausenloy was supported by the British Heart Foundation (CS/14/3/31002); the National Institute for Health Research University College London Hospitals Biomedical Research Centre; Duke-National University Singapore Medical School; Singapore Ministry of Health's National Medical Research Council under its Clinician Scientist-Senior Investigator scheme (NMRC/CSA-SI/0011/2017) and Collaborative Centre Grant scheme (NMRC/CGAug16C006); and the Singapore Ministry of Education Academic Research Fund Tier 2 (MOE2016-T2-2-021). This work was also funded in part by National Health and Medical Research Council project grants (#1057741 and #1139489 to DWG), and Helen Amelia Hanis Fellowship (to DWG). The O'Brien Institute Department of St Vincent's Institute of Medical Research and the Centre for Eye Research Australia receive Operational Infrastructure Support from the Victorian State Government's Department of Innovation, Industry and Regional Development. We thank Charles P. Lai and Bakhos A. Tannous for providing the CSCW-GlucB-IRES-GFP and CSCW-sshBirA-IRES-mCherry plasmids, and Layal Wazen for the generation of the lentiviruses. This article is based upon work from COST

Action EU-CARDIOPROTECTION CA16225 supported by COST (European Cooperation in Science and Technology).

CONFLICT OF INTEREST

None declared

Author contributions: S.Y.L and D.J.H. designed the experiments. R.C.B.W, A.E.N., B.A.T. and T.L. provided materials. A.R.K., D.W.G, A.M.K., P.J.M., H.F, P.S., C.K., L.M., and S.Y.L. performed experiments and collected samples. A.R.K., D.W.G., A.M.K., H.F., R.S., and J.G.L. analyzed the data with guidance from T.L., D.J.H and S.Y.L. D.J.H. and S.Y.L. wrote the manuscript with edits from other authors.

REFERENCES

1. Cabrera-Fuentes HA, Aragones J, Bernhagen J, Boening A, Boisvert WA, Botker HE, Bulluck H, Cook S, Di Lisa F, Engel FB, Engelmann B, Ferrazzi F, Ferdinandy P, Fong A, Fleming I, Gnaiger E, Hernandez-Resendiz S, Kalkhoran SB, Kim MH, Lecour S, Liehn EA, Marber MS, Mayr M, Miura T, Ong SB, Peter K, Sedding D, Singh MK, Suleiman MS, Schnittler HJ, Schulz R, Shim W, Tello D, Vogel CW, Walker M, Li QO, Yellon DM, Hausenloy DJ, Preissner KT. From basic mechanisms to clinical applications in heart protection, new players in cardiovascular diseases and cardiac theranostics: meeting report from the third international symposium on "New frontiers in cardiovascular research". *Basic Res Cardiol* 2016;**111**:69.

2. Madonna R, Van Laake LW, Davidson SM, Engel FB, Hausenloy DJ, Lecour S, Leor J, Perrino C, Schulz R, Ytrehus K, Landmesser U, Mummery CL, Janssens S, Willerson J, Eschenhagen T, Ferdinandy P, Sluijter JP. Position Paper of the European Society of Cardiology Working Group Cellular Biology of the Heart: cell-based therapies for myocardial repair and regeneration in ischemic heart disease and heart failure. *Eur Heart J* 2016;**37**:1789-1798.

3. Zhang M, Methot D, Poppa V, Fujio Y, Walsh K, Murry CE. Cardiomyocyte grafting for cardiac repair: graft cell death and anti-death strategies. *J Mol Cell Cardiol* 2001;**33**:907-921.

4. Hodgkinson CP, Bareja A, Gomez JA, Dzau VJ. Emerging Concepts in Paracrine Mechanisms in Regenerative Cardiovascular Medicine and Biology. *Circ Res* 2016;**118**:95-107.

5. Peng Y, Pan W, Ou Y, Xu W, Kaelber S, Borlongan CV, Sun M, Yu G. Extracardiac-Lodged Mesenchymal Stromal Cells Propel an Inflammatory Response Against Myocardial Infarction via Paracrine Effects. *Cell transplantation* 2016;**25**:929-935.

6. Zhang Y, Sivakumaran P, Newcomb AE, Hernandez D, Harris N, Khanabdali R, Liu GS, Kelly DJ, Pebay A, Hewitt AW, Boyle A, Harvey R, Morrison WA, Elliott DA, Dusting GJ, Lim SY. Cardiac Repair With a Novel Population of Mesenchymal Stem Cells Resident in the Human Heart. *Stem Cells* 2015;**33**:3100-3113.

7. Nie S, Wang X, Sivakumaran P, Chong MMW, Liu X, Karnezis T, Bandara N, Takov K, Nowell CJ, Wilcox S, Shambrook M, Hill AF, Harris NC, Newcomb AE, Strappe P, Shayan R, Hernandez D, Clarke J, Hanssen E, Davidson SM, Dusting GJ, Pebay A, Ho JWK, Williamson N, Lim SY. Biologically active constituents of the secretome of human W8B2(+) cardiac stem cells. *Sci Rep* 2018;**8**:1579.

8. Lai CP, Mardini O, Ericsson M, Prabhakar S, Maguire C, Chen JW, Tannous BA, Breakefield XO. Dynamic biodistribution of extracellular vesicles in vivo using a multimodal imaging reporter. *ACS Nano* 2014;**8**:483-494.

9. Thul PJ, Akesson L, Wiking M, Mahdessian D, Geladaki A, Ait Blal H, Alm T, Asplund A, Bjork L, Breckels LM, Backstrom A, Danielsson F, Fagerberg L, Fall J, Gatto L, Gnann C, Hober S, Hjelmare M, Johansson F, Lee S, Lindskog C, Mulder J, Mulvey CM, Nilsson P, Oksvold P, Rockberg J, Schutten R, Schwenk JM, Sivertsson A, Sjostedt E, Skogs M, Stadler C, Sullivan DP, Tegel H, Winsnes C, Zhang C, Zwahlen M, Mardinoglu A, Ponten F, von Feilitzen K, Lilley KS, Uhlen M, Lundberg E. A subcellular map of the human proteome. *Science* 2017;**356**.

10. Doll S, Dressen M, Geyer PE, Itzhak DN, Braun C, Doppler SA, Meier F, Deutsch MA, Lahm H, Lange R, Krane M, Mann M. Region and cell-type resolved quantitative proteomic map of the human heart. *Nat Commun* 2017;**8**:1469.

11. Tibell A, Rafael E, Wennberg L, Nordenstrom J, Bergstrom M, Geller RL, Loudovaris T, Johnson RC, Brauker JH, Neuenfeldt S, Wernerson A. Survival of macroencapsulated allogeneic parathyroid tissue one year after transplantation in nonimmunosuppressed humans. *Cell Transplant* 2001;**10**:591-599.

12. Tarantal AF, Lee CC, Itkin-Ansari P. Real-time bioluminescence imaging of macroencapsulated fibroblasts reveals allograft protection in rhesus monkeys (Macaca mulatta). *Transplantation* 2009;**88**:38-41.

13. Motte E, Szepessy E, Suenens K, Stange G, Bomans M, Jacobs-Tulleneers-Thevissen D, Ling Z, Kroon E, Pipeleers D. Composition and function of macroencapsulated human embryonic stem cell-derived implants: comparison with clinical human islet cell grafts. *Am J Physiol Endocrinol Metab* 2014;**307**:E838-846.

14. Loudovaris T, Jacobs S, Young S, Maryanov D, Brauker J, Johnson RC. Correction of diabetic nod mice with insulinomas implanted within Baxter immunoisolation devices. *J Mol Med (Berl)* 1999;**77**:219-222.

15. Josephs SF, Loudovaris T, Dixit A, Young SK, Johnson RC. In vivo delivery of recombinant human growth hormone from genetically engineered human fibroblasts implanted within Baxter immunoisolation devices. *J Mol Med (Berl)* 1999;**77**:211-214.

16. Yanay O, Barry SC, Flint LY, Brzezinski M, Barton RW, Osborne WR. Long-term erythropoietin gene expression from transduced cells in bioisolator devices. *Hum Gene Ther* 2003;**14**:1587-1593.

17. Whyte W, Roche ET, Varela CE, Mendez K, Islam S, O'Neill H, Weafer F, Shirazi RN, Weaver JC, Vasilyev NV, McHugh PE, Murphy B, Duffy GP, Walsh CJ, Mooney DJ. Sustained release of targeted cardiac therapy with a replenishable implanted epicardial reservoir. *Nat Biomed Eng* 2018;**2**:416-428.

18. Shirazi RN, Islam S, Weafer FM, Whyte WD, Varela CE, Villanyi A, Ronan W, McHugh P, Roche ET. Multiscale Experimental and Computational Modeling Approaches to Characterize Therapy Delivery to the Heart from an Implantable Epicardial Biomaterial Reservoir. *Adv Healthc Mater* 2019:e1900228.

19. Johnston PV, Hwang CW, Bogdan V, Mills KJ, Eggan ER, Leszczynska A, Wu KC, Herzka DA, Brinker JA, Schulman SP, Banerjee M, Florea V, Natsumeda M, Tompkins B, Balkan W, Hare JM, Tomaselli GF, Weiss RG, Gerstenblith G. Intravascular Stem Cell Bioreactor for Prevention of Adverse Remodeling After Myocardial Infarction. *J Am Heart Assoc* 2019;**8**:e012351.

20. Vagnozzi RJ, Maillet M, Sargent MA, Khalil H, Johansen AKZ, Schwanekamp JA, York AJ, Huang V, Nahrendorf M, Sadayappan S, Molkentin JD. An acute immune response underlies the benefit of cardiac stem cell therapy. *Nature* 2020;**577**:405-409.

21. Davidson SM, Takov K, Yellon DM. Exosomes and Cardiovascular Protection. *Cardiovasc Drugs Ther* 2017;**31**:77-86.

22. Ju C, Shen Y, Ma G, Liu Y, Cai J, Kim IM, Weintraub NL, Liu N, Tang Y. Transplantation of Cardiac Mesenchymal Stem Cell-Derived Exosomes Promotes Repair in Ischemic Myocardium. *J Cardiovasc Transl Res* 2018;**11**:420-428.

23. Ibrahim AG, Cheng K, Marban E. Exosomes as critical agents of cardiac regeneration triggered by cell therapy. *Stem Cell Reports* 2014;**2**:606-619.

24. Wang Y, Zhang L, Li Y, Chen L, Wang X, Guo W, Zhang X, Qin G, He SH, Zimmerman A, Liu Y, Kim IM, Weintraub NL, Tang Y. Exosomes/microvesicles from induced pluripotent stem cells deliver cardioprotective miRNAs and prevent cardiomyocyte apoptosis in the ischemic myocardium. *Int J Cardiol* 2015;**192**:61-69.

25. Harane NE, Correa BL, Gomez I, Hocine HR, Vilar J, Desgres M, Bellamy V, Keirththana K, Guillas C, Perotto M, Pidial L, Alayrac P, Tran T, Tan S, Hamada T, Charron D, Brisson A, Renault NK, Al-Daccak R, Menasche P, Silvestre JS. Extracellular Vesicles from Human Cardiovascular Progenitors Trigger a Reparative Immune Response in Infarcted Hearts. *Cardiovascular research* 2020.

26. Lopez E, Blazquez R, Marinaro F, Alvarez V, Blanco V, Baez C, Gonzalez I, Abad A, Moreno B, Sanchez-Margallo FM, Crisostomo V, Casado JG. The Intrapericardial Delivery

of Extracellular Vesicles from Cardiosphere-Derived Cells Stimulates M2 Polarization during the Acute Phase of Porcine Myocardial Infarction. *Stem Cell Rev Rep* 2019.

27. Jiang S, Hamakubo T, Mitsui K, Yagami R, Fujiyoshi Y, Ajioka Y, Naito M. Roundabout1 distribution in neoplastic and non-neoplastic diseases with a focus on neoangiogenesis. *Int J Clin Exp Pathol* 2018;**11**:5755-5764.

28. Zhao L, Ben-Yair R, Burns CE, Burns CG. Endocardial Notch Signaling Promotes Cardiomyocyte Proliferation in the Regenerating Zebrafish Heart through Wnt Pathway Antagonism. *Cell Rep* 2019;**26**:546-554 e545.

29. Xu R, Rai A, Chen M, Suwakulsiri W, Greening DW, Simpson RJ. Extracellular vesicles in cancer - implications for future improvements in cancer care. *Nat Rev Clin Oncol* 2018;**15**:617-638.

30. Xu R, Greening DW, Chen M, Rai A, Ji H, Takahashi N, Simpson RJ. Surfaceome of Exosomes Secreted from the Colorectal Cancer Cell Line SW480: Peripheral and Integral Membrane Proteins Analyzed by Proteolysis and TX114. *Proteomics* 2019;**19**:e1700453.

31. Hoshino A, Costa-Silva B, Shen TL, Rodrigues G, Hashimoto A, Tesic Mark M, Molina H, Kohsaka S, Di Giannatale A, Ceder S, Singh S, Williams C, Soplop N, Uryu K, Pharmer L, King T, Bojmar L, Davies AE, Ararso Y, Zhang T, Zhang H, Hernandez J, Weiss JM, Dumont-Cole VD, Kramer K, Wexler LH, Narendran A, Schwartz GK, Healey JH, Sandstrom P, Labori KJ, Kure EH, Grandgenett PM, Hollingsworth MA, de Sousa M, Kaur S, Jain M, Mallya K, Batra SK, Jarnagin WR, Brady MS, Fodstad O, Muller V, Pantel K, Minn AJ, Bissell MJ, Garcia BA, Kang Y, Rajasekhar VK, Ghajar CM, Matei I, Peinado H, Bromberg J, Lyden D. Tumour exosome integrins determine organotropic metastasis. *Nature* 2015;**527**:329-335.

32. Gao L, Mei S, Zhang S, Qin Q, Li H, Liao Y, Fan H, Liu Z, Zhu H. Cardio-renal Exosomes in Myocardial Infarction Serum Regulate Proangiogenic Paracrine Signaling in Adipose Mesenchymal Stem Cells. *Theranostics* 2020;**10**:1060-1073.

33. Teoh SL, Das S. Notch Signalling Pathways and Their Importance in the Treatment of Cancers. *Curr Drug Targets* 2018;**19**:128-143.

FIGURE LEGENDS

Figure 1. Subcutaneous implantation of W8B2$^+$ CSCs encapsulated in a TheraCyte device induces cardioprotection in a rat model of myocardial infarction. (A) Schematic of W8B2$^+$ CSCs encapsulated in a TheraCyte device. (B) Representative M-mode view of echocardiography at 4 weeks following myocardial infarction and summarized mean data of ejection fraction (EF) (n = 6-7). (C) Representative images of left ventricular cross-sections stained with Masson's trichrome and infarct size expressed as the percentage of fibrotic scar area over total left ventricle. (D) Representative images of collagen fibers (in red) stained with picrosirius red and percentage of interstitial fibrosis in the remote myocardium. (E) Representative images of left ventricular cross-sections stained with wheat germ agglutinin and the relative cross-sectional area of cardiomyocytes. (F) Total vascular density determined in lectin-stained sections. (G) Arteriole density determined in smooth muscle actin-stained sections. n = 7-8. Data are shown as mean ± SEM. *P < 0.05, **P < 0.01, ***P < 0.001 versus control by unpaired Student's *t* test or by two-way ANOVA with Bonferroni post-hoc test in (B).

Figure 2. Encapsulated W8B2$^+$ CSCs in TheraCyte devices. (A-B) Eosin-haematoxylin stained Theracyte sections at 0 (A) and 4 (B) weeks post-implantation. (C-E) TheraCyte devices with encapsulated W8B2$^+$ CSCs at 4 weeks post-implantation and stained with human-specific KU80 antibody (C), lectin (D, arrows indicate erythrocytes), cleaved caspase-3 antibody (E) and Ki67 antibody (F). (E) The percentage of cell area within the TheraCyte stained positive for cleaved caspase-3 (arrows) at day 28 post-implantation. n = 7. (F) The percentage of Ki67 positive cells (arrows) encapsulated within the TheraCyte devices at day 28 post-implantation. n = 7.

Figure 3. Characterisation of extracellular vesicles secreted by encapsulated W8B2$^+$ CSCs. (A) Transduced W8B2+ cells expressing both the GlucB-IRES-GFP and sshBirA-IRES-mCherry vectors (W8B2$^+$ CSC$^{GlucB+sshBirA}$), resulting in extracellular vesicles with GlucB and sshBirA

labelled and biotinylated on the surface of the plasma membrane. (B) W8B2$^+$ CSC$^{GlucB+sshBirA}$ encapsulated within a TheraCyte device and expressing mCherry and GFP fluorescence proteins *in vitro*. (C-D) Gluc activity (C) and concentration (D) of microvesicles in conditioned media (50 µL and centrifuged at 500*g*) harvested at 1, 2 and 3 days from W8B2$^+$ CSC$^{GlucB+sshBirA}$ cultured as monolayer (2D) or encapsulated within a TheraCyte device (3D). n = 3 independent experiments. Data are shown as mean ± SEM. *P < 0.05, ****P < 0.0001 by one-way ANOVA with Bonferroni post-hoc test. (E-F) Nanoparticle tracking analysis showing the size distribution of EVs in conditioned media harvested at 1, 2 and 3 days from W8B2$^+$ CSC$^{GlucB+sshBirA}$ cultured as monolayer (E) or encapsulated within a TheraCyte device (F). (G) Size distribution of EVs in conditioned media harvested on day-3 (~1.5 mL and centrifuged at 2,000g followed by 110,000*g* twice) from untransduced W8B2$^+$ CSCs and W8B2$^+$ CSC$^{GlucB+sshBirA}$ encapsulated within a TheraCyte device. n = 3 independent experiment.

Figure 4. Characterisation of extracellular vesicles secreted by W8B2$^+$ CSCs. (A) PCA analysis of proteins identified in untransduced cells (UnT Cell), matched EVs (UnT EV), and transduced EVs (T EV). Unsupervised PCA analysis wass conducted using the average protein LFQ intensities of technical replicates. Correlation matrix was visualised with illustrated pearson correlation coefficient using psych package in R. (B) Volcano plot, statistically significant proteins with less than 0.05 adjusted p-value and greater than 1.5 log2 fold change differences. (C) Exosome marker proteins identified and enriched in UnT EV and T EV relative to UnT cells. (D) Distribution of protein identified between UnT EV and T EV. (E) Multi-variate analysis of intra- (technical) and inter (biological) sample variation of UnT EV and T EV. (F-G) KEGG functional enrichment analysis of UnT EV, reveals significant enrichment, relative to human genome (p<0.01), of the ROBO receptor signalling (HSA-376176) (F) and NOTCH signalling (HSA-157118) (G).

Figure 5. Biodistribution of extracellular vesicles secreted by encapsulated W8B2^{+} CSCs. (A-B) W8B2^{+} CSC$^{GlucB+sshBirA}$ encapsulated within a TheraCyte device were implanted subcutaneously into rats following myocardial infarction. At 4 weeks post-implantation, paraffin-embedded sections were stained with horseradish peroxidase-conjugated streptavidin to detect biotin (A) or with GFP antibody (B) showing positive punctate staining around across the inner membrane and in cells within the vicinity of the TheraCyte device (arrows). (C-D) Cryosections of the myocardium showed retention of extracellular vesicles of W8B2^{+} CSC$^{GlucB+sshBirA}$ (arrows) in the interstitial space and inside the cardiomyocytes (C), as well as in the peri-vascular region (D). The super-resolution confocal images are the enlarged views of the field covered by the white boxes shown in the confocal images.

Graphical Abstract: Sustained subcutaneous delivery of proteins secreted by stem cells to repair damaged hearts.

Figure 1

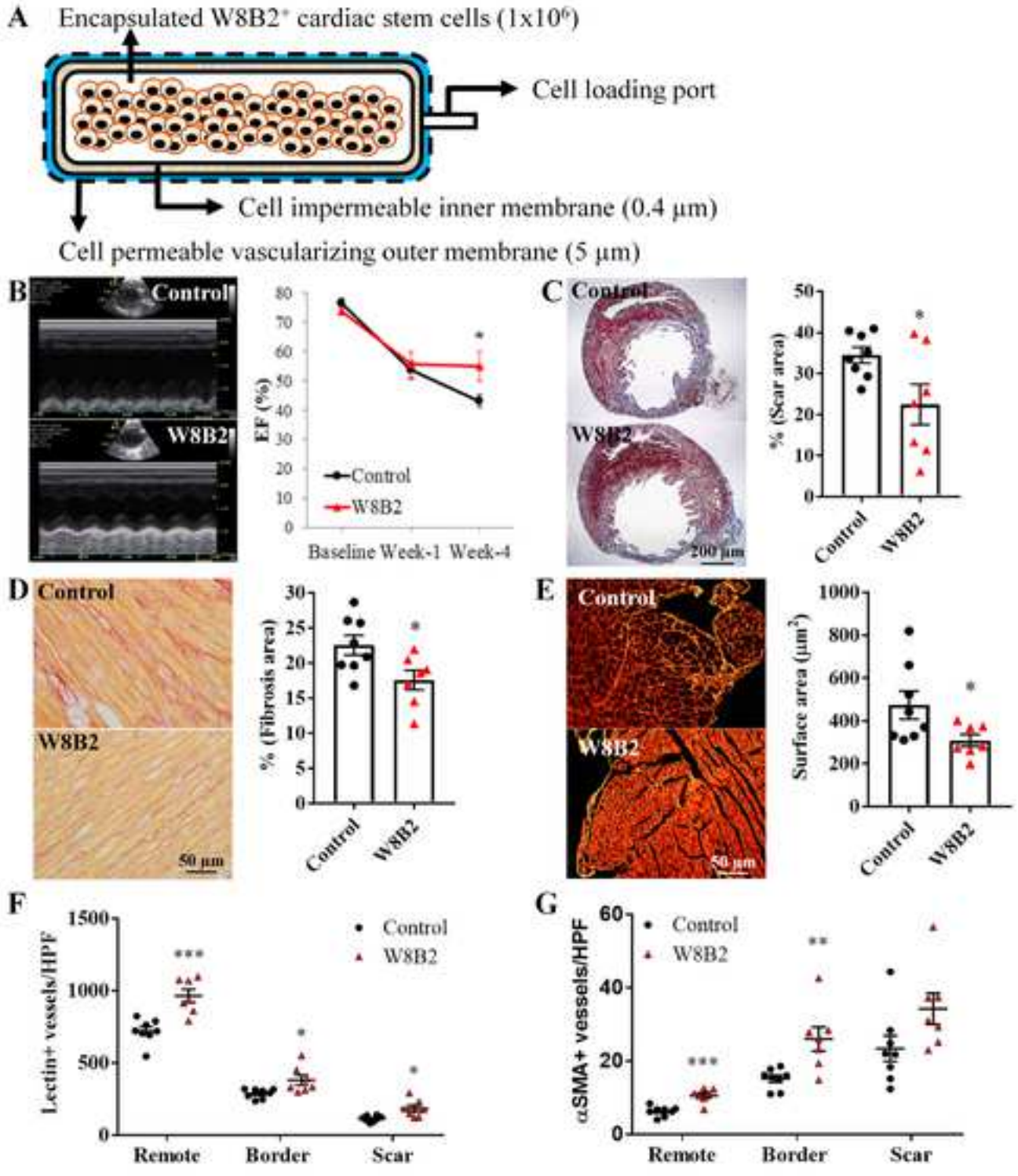

Figure 2

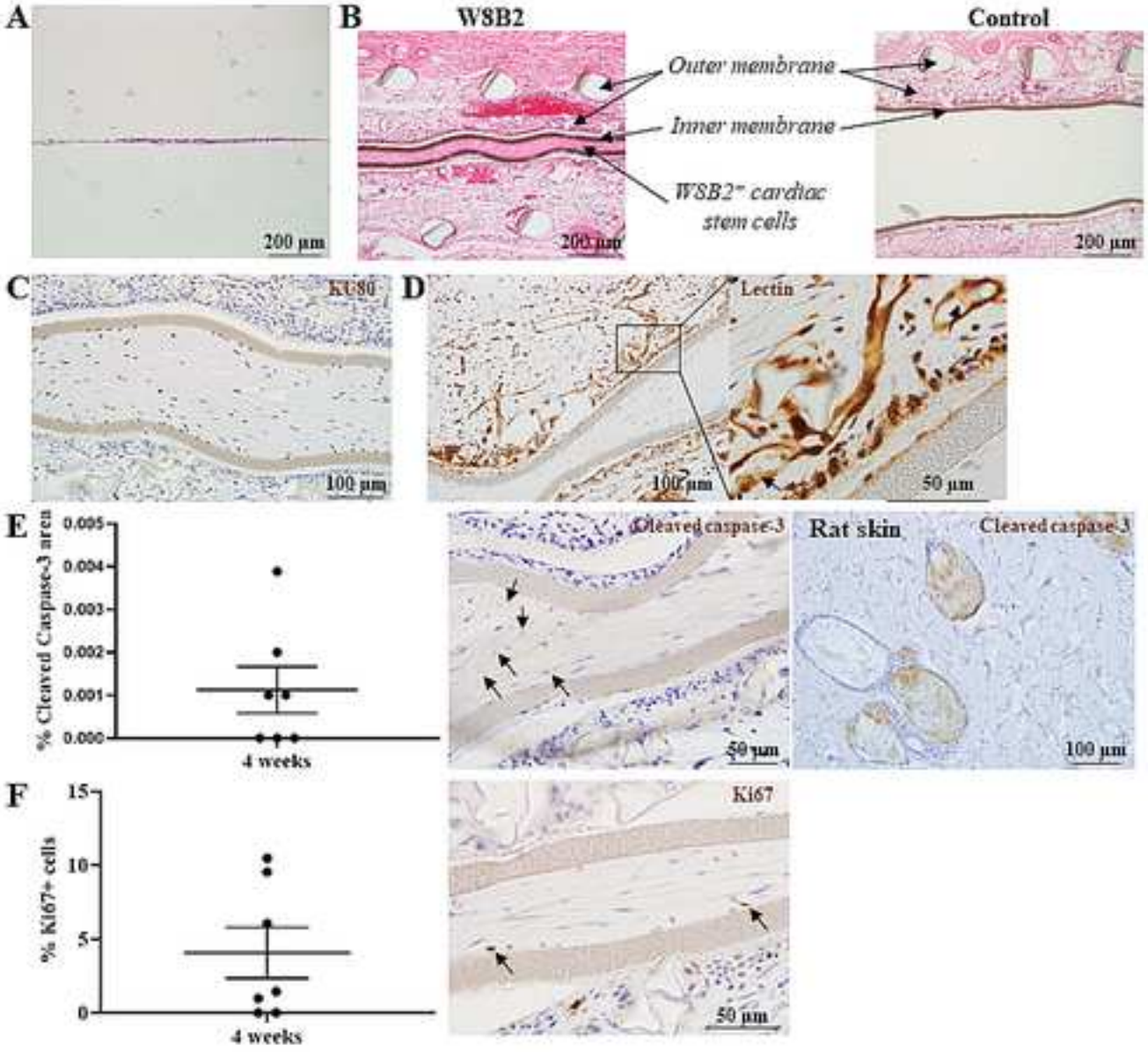

Figure 3

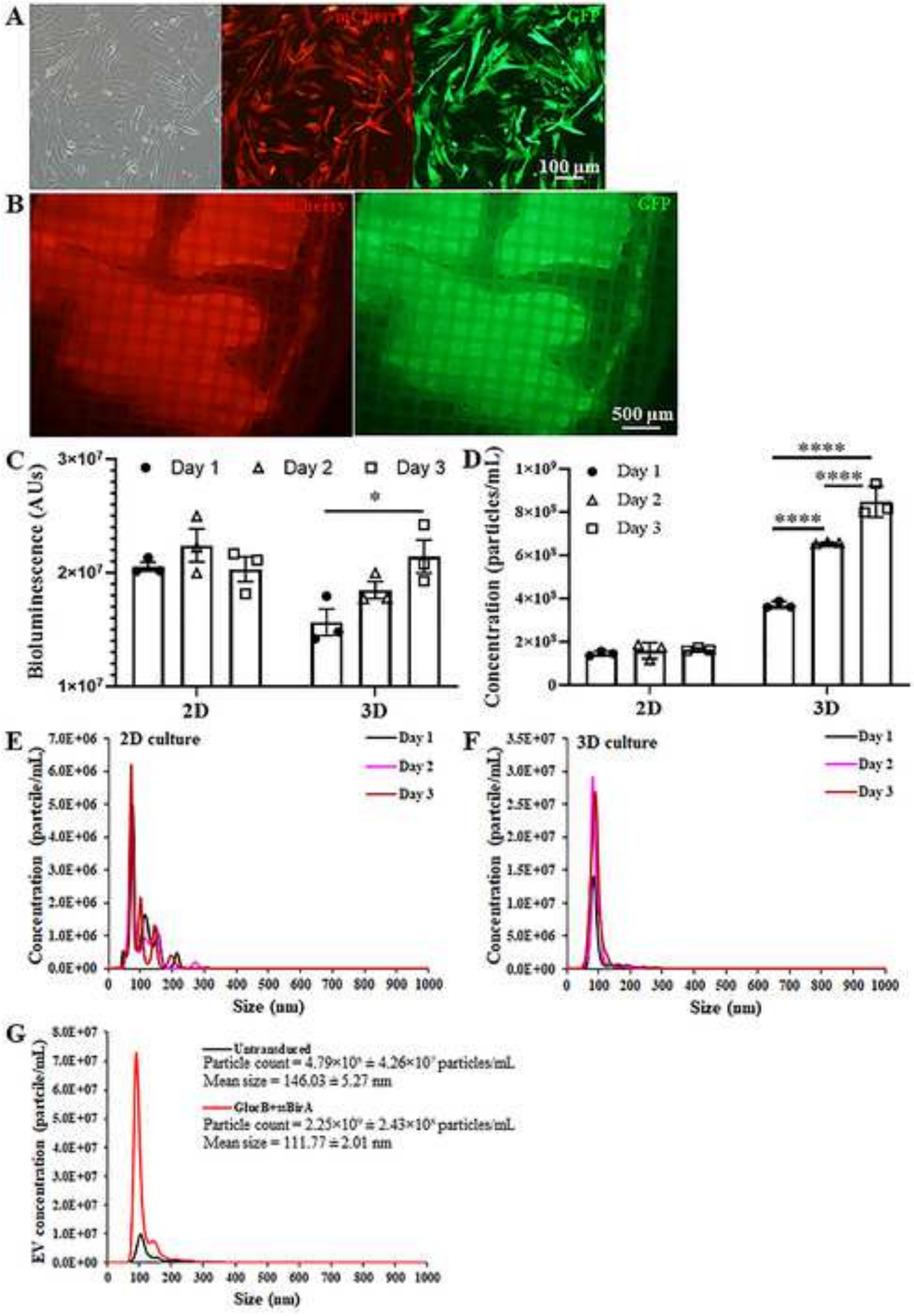

Figure 4

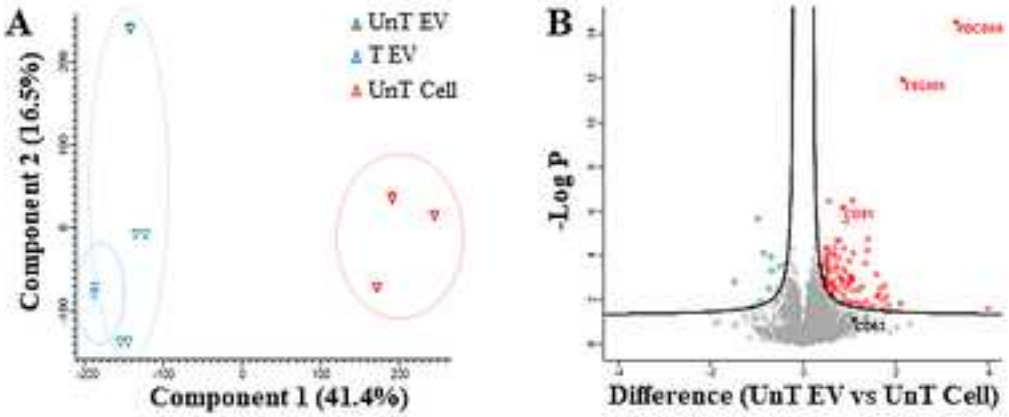

C

Protein Accession	Gene Name	Protein Name	Cell (AVG)	UnT EV (AVG)	Reporter (T) EV (AVG)	Fold change (UnT EV vs Cell)	Fold change (UnT EV vs T EV)
P08962	CD63	CD63 antigen	24.5	25.6	26.1	1.1	0.5
Q8WUM4	PDCD6IP	Programmed cell death 6-interacting protein	25.1	28.4	28.5	3.3	0.0
Q99816	TSG101	Tumor susceptibility gene 101 protein	23.8	26.0	25.9	2.1	0.0
P60033	CD81	CD81 antigen	25.7	26.5	26.3	0.9	-0.2

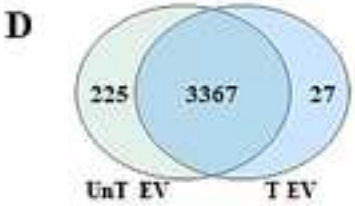

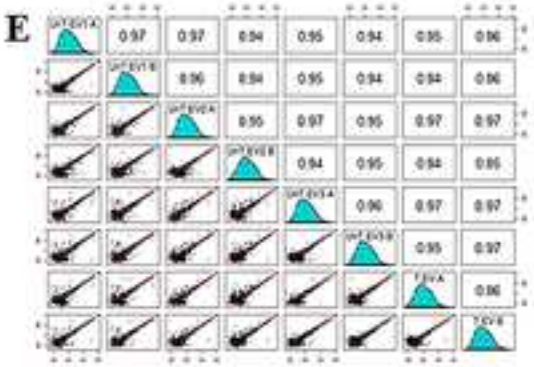

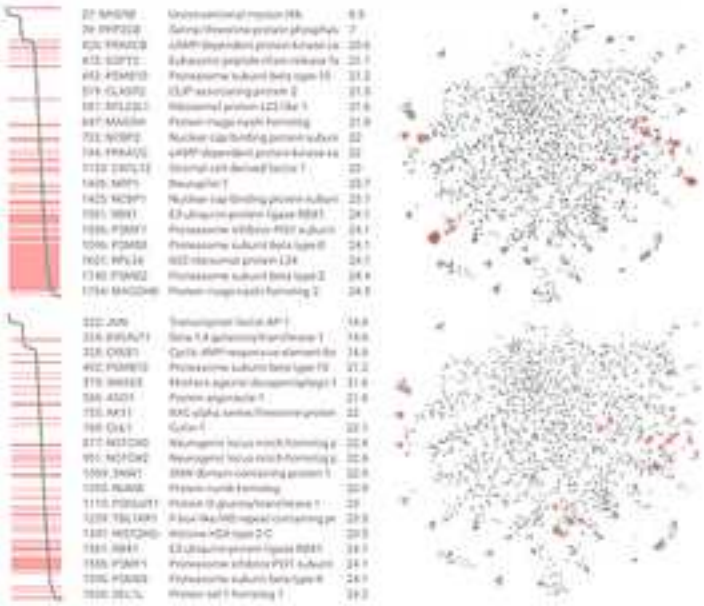

Figure 5

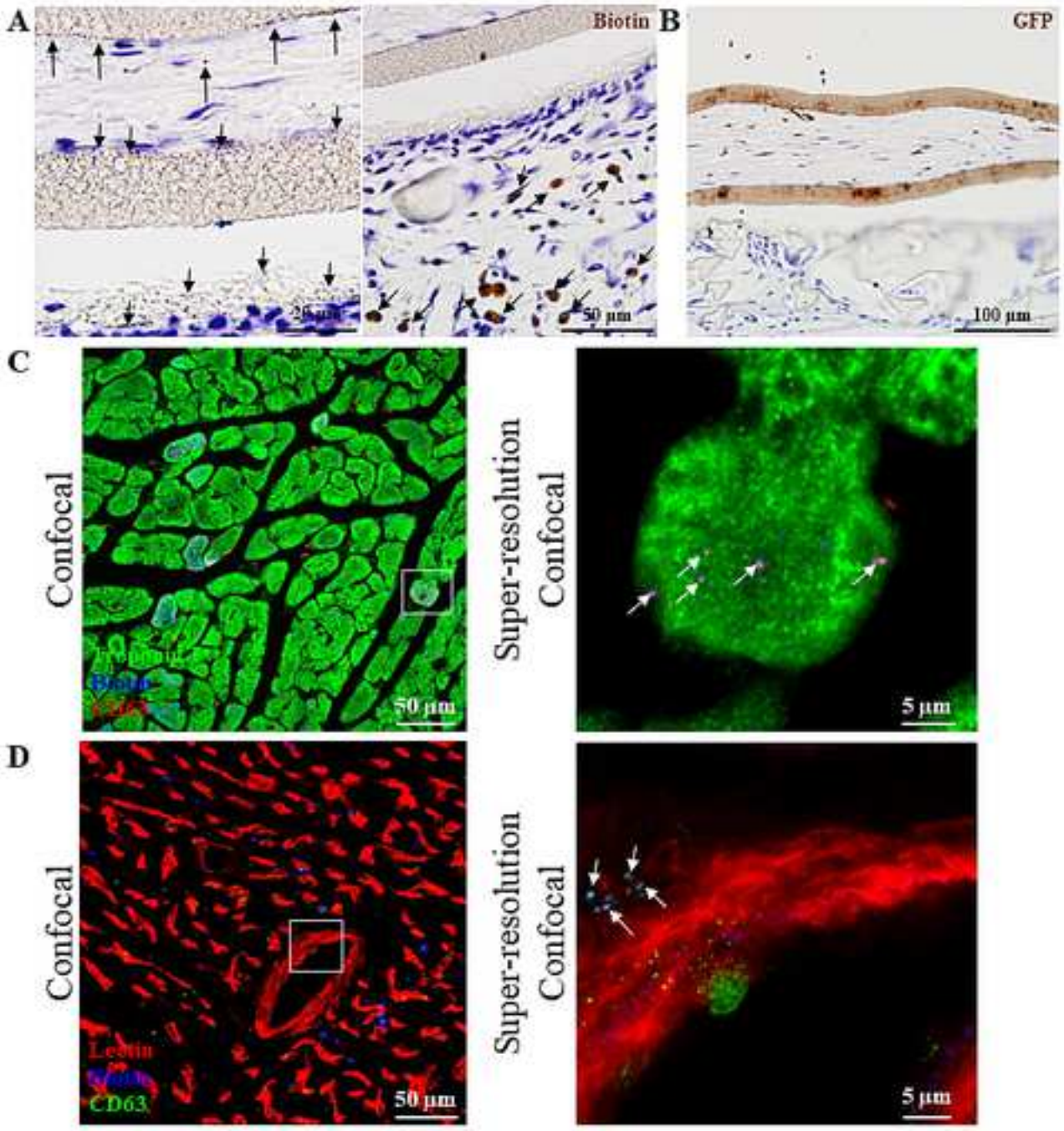

Graphical abstract